Article:
Zhao, Y, Ni, X, Ye, S orcid.org/0000-0001-5152-5753 et al. (3 more authors) (2020) A Smart Route for Encapsulating Pd Nanoparticles into a ZIF-8 Hollow Microsphere and Their Superior Catalytic Properties. Langmuir, 36 (8). pp. 2037-2043. ISSN 0743-7463

https://doi.org/10.1021/acs.langmuir.9b03731

LANGMUIR

Interface Components: Nanoparticles, Colloids, Emulsions, Surfactants, Proteins, Polymers

A smart route for encapsulating Pd nanoparticles into a ZIF-8 hollow microsphere and their superior catalytic properties

Yaqian Zhao, Xinjiong Ni, Sunjie Ye, Zhi-Guo Gu, Yunxing Li, and To Ngai

Langmuir, **Just Accepted Manuscript** • DOI: 10.1021/acs.langmuir.9b03731 • Publication Date (Web): 09 Feb 2020

A smart route for encapsulating Pd nanoparticles into a ZIF-8 hollow microsphere and their superior catalytic properties

Yaqian Zhao[a], Xinjiong Ni[a], Sunjie Ye[b], Zhi-Guo Gu[a], Yunxing Li[a,], and To Ngai[c,]**

[a] Key Laboratory of Synthetic and Biological Colloids, Ministry of Education, School of Chemical and Material Engineering, Jiangnan University, Wuxi 214122, China

[b] School of Physics and Astronomy, University of Leeds, Leeds, LS2 9JT, UK

[c] Department of Chemistry, The Chinese University of Hong Kong, Shatin, N. T., Hong Kong

ABSTRACT

The encapsulation of catalytically-active noble metal nanoparticles into metal-organic frameworks (MOFs) represents an effective strategy for enhancing their catalytic performance. Despite a myriad of reports on the nanocomposites consisting of noble metal nanoparticles and MOFs, it remains challenging to develop a sustainable and convenient method for realizing confined integration of noble metal nanoparticles within a porous and hollow zinc-based MOF. Herein a simple and well-designed approach is reported to the fabrication of Pd@ZIF-8 hollow microspheres with a number of Pd nanoparticles immobilized on the inner surface. This method

capitalized on the use of polyvinylpyrrolidone (PVP) stabilized polystyrene (PS) microspheres as templates, to harness the dual functions of PVP for reducing $PdCl_2$ to generate Pd NPs and coordinating with zinc ions to grow ZIF-8 shell. Consequently, it avoids the complicated protocols involving surface treatment of template microspheres that conventionally adopts hazardous or costly agents. The obtained Pd@ZIF-8 hollow microspheres exhibit outstanding catalytic activity, size selectivity, and stability in the hydrogenation of alkenes. This study presents both the advances in the green synthesis and great potential of Pd@ZIF-8 hollow microspheres for catalytic applications.

KEYWORDS: palladium nanoparticle; ZIF-8; encapsulation; hollow microsphere; catalysis

INTRODUCTION

The development of noble metal nanoparticles (NM NPs) as catalyst has received increasing attention because of their unique catalytic functions in various chemical reactions, but the improvement of their catalytic performance (activity, stability and selectivity) by a convenient and controllable method remains a great challenge.[1, 2] To this end, the hybridization of NM NPs with metal-organic frameworks (MOFs) has emerged as a rational route that has stimulated considerable research interest, because (1) the catalytic activity can be enhanced by the confinement effect of MOF cavity that builds up local concentrations of reactants, as well as the synergy of the MOF shell and incorporated NM NPs; (2) the catalytic selectivity can be achieved by the modulation of the diameter and surface properties (hydrophilic or hydrophobic) of pores in the shell of MOFs, that enables selective and fast diffusion of reaction reagents through the interior cavities, especially for reactions in liquid phase; (3) the stability can be improved due to the porous shell of MOFs, that can reduce undesirable aggregation and atomic leaching of NM NPs.[3-9] However, it is challenging to encapsulate well-dispersed NM NPs into MOFs, and the resultant structures tend to suffer from nonuniform morphologies with NM NP aggregates inside the MOFs or NM NPs exposed on the external surface of MOFs.[10]

Up to now, there have been few reports on the confined incorporation of many NM NPs within one MOF hollow microsphere (NM@MOF hollow microsphere). Chen's group pioneeringly used Cu_2O particles as a template to achieve the incorporation of Au NPs within the HKUST-1 hollow particles.[11] In contrast to HKUST-1, ZIF-8 has superior thermal stability as well as higher chemical resistance against aqueous and organic solvents, thus is considered as a better candidate to be combined with NM NPs for potential catalytic applications.[12-14] Song's group reported the encapsulation of Pd NPs into ZIF-8 hollow particles using the polystyrene (PS) particles as a

template.[15] This method involves a surface activation of PS template particles by using $SnCl_2$, which subsequently acts as a reductant for the growth of Pd NPs in situ. Both $SnCl_2$ and the product $SnCl_4$ (which was used as a chemical warfare agent in World War I) have posed serious concerns regarding potential biological and environmental risks.[16-18] Therefore, it is considerably desirable to develop green and simple methods for fabricating NM@MOF nanoarchitectures as advanced catalysts.

Herein we report a sustainable and rationally-designed approach to fabricate the Pd@ZIF-8 hollow microspheres with Pd NPs evenly distributed on the inner surface of the ZIF-8 shell. The preparation process relies on dual roles of PVP adsorbed on the template microspheres, as a reductant for producing Pd NPs and a nucleation substrate for growing ZIF-8 shell, thus eliminating any surface pre-treatments of template microspheres. The structural parameters of resultant Pd@ZIF-8 hollow microspheres can be readily tailored by our proposed method. The catalysis performance of as-prepared Pd@ZIF-8 hollow microspheres has been tested by using hydrogenation reaction of alkenes.

EXPERIMENTAL SECTION

Materials

Styrene (St), $PdCl_2$, poly(vinylpyrrolidone) (PVP K-30), isopropanol, azodiisobutyronitrile (AIBN), ethyl acetate, methanol, N,N-dimethylformamide (DMF) and $Zn(NO_3)_2{\cdot}6H_2O$ were supplied by Sinopharm Chemical Reagent Co. 1-hexene, cyclohexene, cyclooctene, and 2-methylimidazole were purchased from Energy Chemical Co. Besides St and AIBN, all chemicals of analytical reagent grade were used as received. St of chemical reagent grade was distilled under

vacuum before use. AIBN of chemical reagent grade was purified by recrystallization in 95% ethanol before use. Ultrapure water (18.2 MΩ cm) was used in all experiments.

Synthesis of PS/Pd@ZIF-8 composite particle

First, PS/Pd composite particles were synthesized according to our recent work.[20] Next, $Zn(NO_3)_2 \cdot 6H_2O$ (1.5 mmol) and PS/Pd composite particles (150 mg) were mixed in methanol (75 mL). After stirring for 15 min, 2-methylimidazole (3 mmol) was dissolved in methanol (75 mL) and then added into the above-mentioned mixture. The reaction was allowed to proceed for another two hours at room temperature. The obtained PS/Pd@ZIF-8 composite particles were collected by centrifugation, then washed with methanol several times, and dried at 60 °C in a vacuum.

Synthesis of Pd@ZIF-8 hollow microsphere

PS/Pd@ZIF-8 composite particles (100 mg) were mixed with DMF (50 mL). The resulting mixture was stirred at room temperature for 24 h. The residual solid was washed several times using DMF and methanol in turn by means of centrifugation and redispersion. At last, the product was dried at 60 °C in a vacuum before use.

Synthesis of ZIF-8

3 mmol of 2-methylimidazole and 1.5 mmol of $Zn(NO_3)_2 \cdot 6H_2O$ were added in 150 mL of methanol. After being stirred at room temperature for 2 h, the resultant ZIF-8 was separated out by centrifugation, washed with methanol, and dried at 60 °C in a vacuum.

Catalysis test in hydrogenation of olefins

The catalytic hydrogenations of 1-hexene, cyclooctene, and cyclohexene were performed in ethyl acetate under hydrogen atmosphere (0.1 MPa). In a typical process, the catalyst particles were added to a three-necked round-bottom flask. The residual air in the flask was evacuated by flushing of H_2 for three times. Afterward, 5.0 mL of ethyl acetate, 1 mmol of olefins, and 0.1 mL

n-heptane (internal standard) were introduced into the flask by a degassed syringe. Catalytic reactions were proceeded for 4 h (for 1-hexene and cyclohexene), and 24 h (for cyclooctene), under hydrogen atmosphere at room temperature. At last, the catalyst particles were collected by centrifugation and the rest of liquid was determined by a gas chromatograph containing a flame ionization detector and an FFAP column. On the other hand, the recovered catalyst particles were reused directly in next run for the recycling experiments.

Characterization

Scanning electron microscopy (SEM) images were taken using S-4800 instrument (Hitachi Co., Japan). Elemental mapping was collected on a Tecnai G2 F30 scanning transmission electron microscope (STEM, Thermo Fisher Scientific Co.) operated at 300 kV acceleration voltage. Transmission electron microscopy (TEM) images were obtained on a JEM-2100 equipment (JEOL Co., Japan). Fourier transform infrared (FT-IR) spectra were measured on a Vector 22 FT-IR spectrometer (Bruker Co., Germany). X-ray diffraction (XRD) patterns were collected using a German Bruker-AXS D8 Advance. The Pd content in the sample was analyzed using inductively coupled plasma-optical emission spectrometer (ICP-OES, Agilent 700 Series). N_2 adsorption/desorption isotherm measurements were conducted on ASAP 2020 MP (Micromeritics Instrument Co., USA) at 77 K. Prior to each measurement, each sample was activated for 6 h at 200 °C in a vacuum.

RESULTS AND DISCUSSION

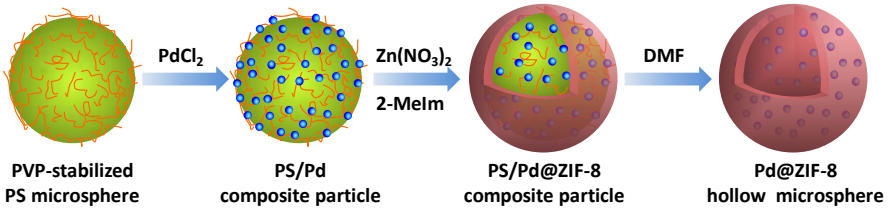

Scheme 1. Schematic representation of the synthetic procedure for the fabrication of Pd@ZIF-8 hollow microsphere.

Scheme 1 represents the synthetic process of Pd@ZIF-8 hollow microspheres. The PVP-stabilized PS microspheres were synthesized via a common dispersion polymerization and adopted as template. After the resulting polymer microspheres were introduced to a $PdCl_2$ aqueous solution at 80 ºC, the highly dispersed Pd NPs were generated on PS microspheres in situ (PS/Pd composite particles), owing to the reducing property of PVP as well as its affinity with Pd NPs.[19, 20] Afterwards, the ZIF-8 shell of desired thickness was formed on the PS microspheres to encapsulate Pd NPs in between PS microspheres and ZIF-8 shell, by using the zinc nitrate and 2-methylimidzole as precursors (PS/Pd@ZIF-8 composite particles).[12] This can be readily achieved because the coordination interaction between zinc ions and carbonyl group (C=O) of pyrrolidone ring in PVP enables the ZIF-8 to effectively deposit on the PS microspheres.[12, 21] Accordingly, additional functionalization or modification of PS template microspheres to provide favorable depositions of Pd NPs and ZIF-8 shell were eliminated. Finally, the PVP-stabilized PS template microspheres were easily removed by DMF.[22] As a result, well-defined Pd@ZIF-8 hollow microspheres were obtained.

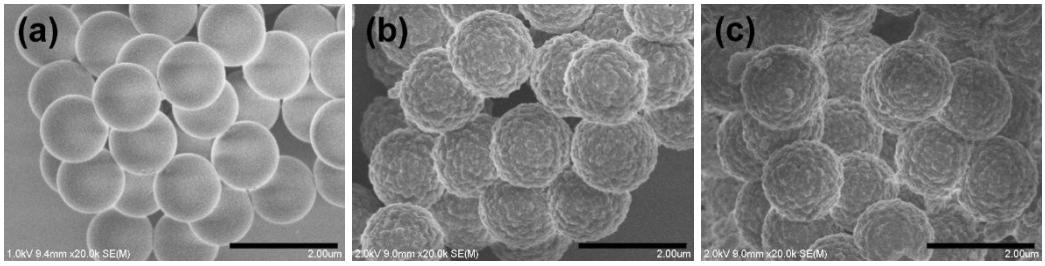

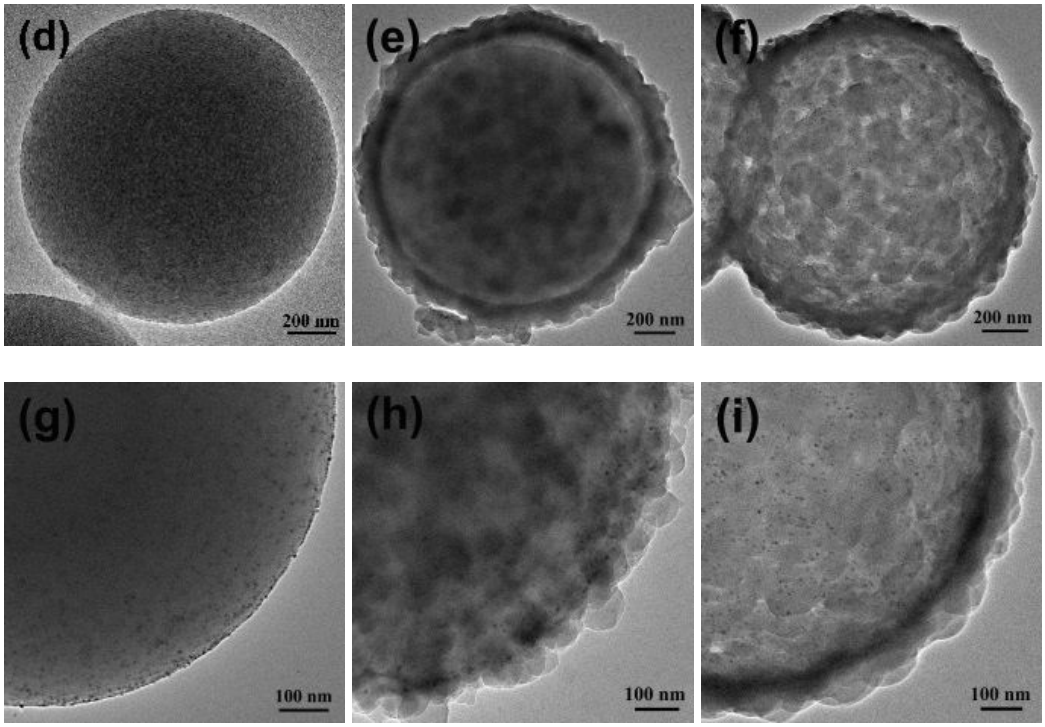

Figure 1. SEM and TEM images for PS/Pd (a, d, g) and PS/Pd@ZIF-8 composite particles (b, e, h) and Pd@ZIF-8 hollow microspheres (c, f, i).

Figure 1 shows typical SEM and TEM images obtained after each step of our preparation process. The PS template microspheres were nearly monodisperse and exhibited an average size around 1.3 μm (Figure S1). After the formation of PS/Pd nanocomposite particles, the TEM image demonstrates a number of dark spots corresponding to small Pd NPs (*ca.* 4.5 nm) that were well dispersed on the PS template microspheres (Figure 1d and 1g).[20] However, the SEM image (Figure 1a) reveals a surface morphology similar to the template microspheres. In contrast, the SEM image (Figure 1b) of the PS/Pd@ZIF-8 composite particles manifests that, each PS/Pd composite particle is encapsulated by a ZIF-8 shell containing some distinguishable rhombic dodecahedron nanocrystal.[22, 23] Further observation by TEM also indicates that the surface of PS/Pd composite particles are uniformly deposited by a shell of ZIF-8 having an average thickness of *ca.* 120 nm (Figure 1e and 1h). Significantly, as can be seen in Figure. 1c, the as-prepared Pd@ZIF-8 hollow

microspheres have an excellent structural integrity and retain well-defined spherical morphology and uniform size. Also, the hollow structure can be clearly confirmed by TEM images that shows a remarkable contrast of the light inner part and the dark margin (Figure 1f and 1i). Furthermore, the removal of polymer template microspheres can be proved by the FTIR spectroscopy. In contrary to the presence of characteristic absorption of ZIF-8, the absorption peaks of PS microspheres completely disappeared in the case of Pd@ZIF-8 hollow microspheres (Figure S2).[24] In addition, Figure 1i clearly suggests the encapsulation of highly dispersed Pd NPs within the ZIF-8 hollow microspheres. The Pd NPs possess an average diameter of about 4.7 nm, close to their original size (Figure 1g). In other words, the aggregation of Pd NPs in our preparation process can be effectively restricted, which is crucial for their catalytic applications.

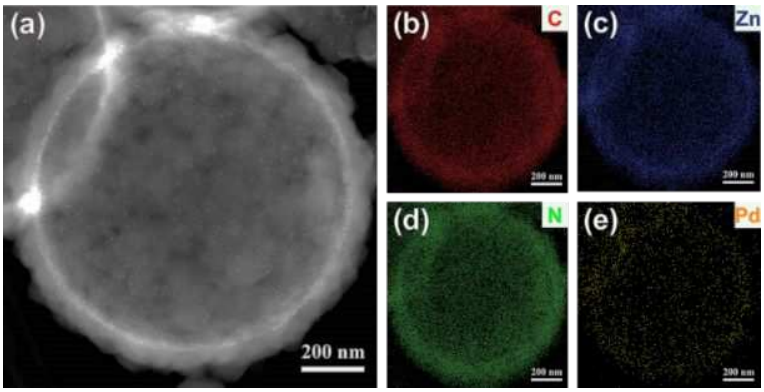

Figure 2. STEM image (a) of Pd@ZIF-8 hollow microsphere and EDX elemental mappings (b-e) showing the distribution of C (red), Zn (blue), N (green) and Pd (yellow).

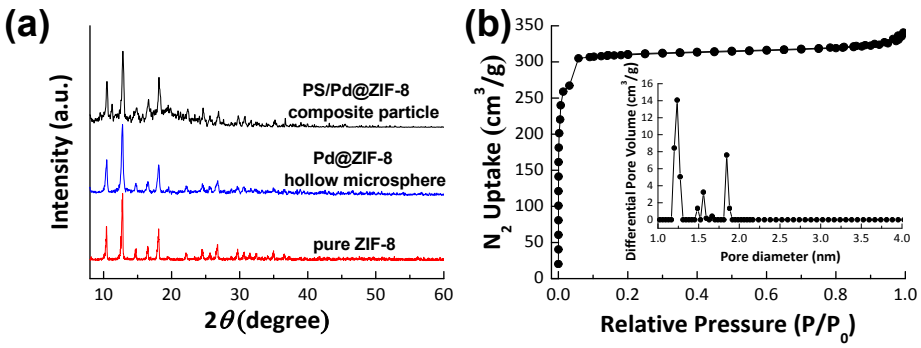

Figure 3. (a) XRD patterns of PS/Pd@ZIF-8 composite particles, Pd@ZIF-8 hollow microspheres and pure ZIF-8, respectively; (b) Nitrogen adsorption/desorption isotherms of Pd@ZIF-8 hollow microspheres with inset showing the pore size distribution.

The structure and composition of the as-prepared Pd@ZIF-8 hollow microspheres were further characterized by the EDX elemental mapping, XRD, ICP-OES, and nitrogen adsorption/desorption. A close inspection of STEM image (Figure 2a) reveals the uniform distribution of many white spots corresponding to Pd NPs.[25] Furthermore, the elements of C, N, Zn, and Pd display more dense distribution on the periphery region than at the center area, substantiating the hollow structure and composition of the as-prepared product.[11] The sharp diffraction peaks in the XRD pattern of the Pd@ZIF-8 hollow microspheres (Figure 3a), agreed with those of pure ZIF-8, which indicated that the crystalline structure of ZIF-8 was formed and well preserved.[26, 27] The characteristic peaks of the Pd NPs are not detectable, which may be due to their small size, high dispersity, and low mass loading.[28, 29] The ICP-OES result shows the content of Pd element inside the Pd@ZIF-8 hollow microspheres is just about 1.86%. In Figure. 3b, the nitrogen adsorption/desorption isotherms of Pd@ZIF-8 hollow microspheres exhibit a type Ⅰ behavior. The steep increase in nitrogen uptake at a low relative pressure is similar to that of pristine ZIF-8 (Figure S3), indicating the ZIF-8 shell has a microporous structure.[13] The size distribution of micropores is ranging from 1 to 2 nm (inset in Figure 3b). Furthermore, the BET surface area of obtained Pd@ZIF-8 hollow microspheres has been measured to be 927 m^2/g, lower than that of pristine ZIF-8 (1269 m^2/g). The reduced surface area is attributable to the presence of heavier and nonporous Pd NPs.[30] However, this slight decrease in BET surface area suggests that the presence of Pd NPs has not effectively blocked the pores of ZIF-8 and thus not affects the transportation of reactants with given size in catalytic reactions.

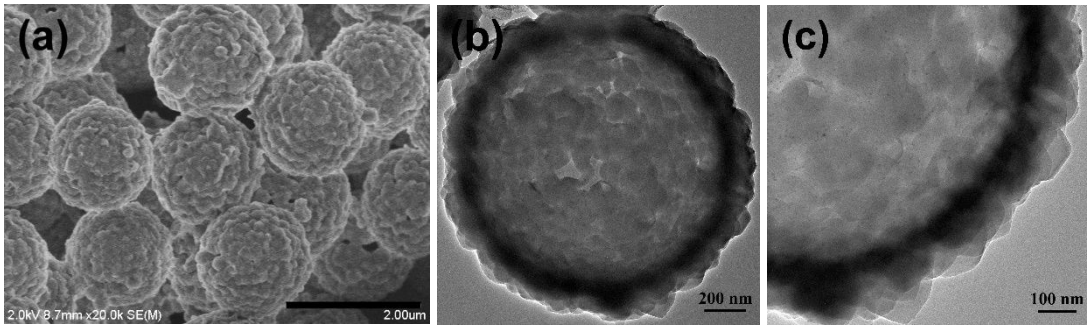

Figure 4. SEM image (a) and TEM images (b and c) of the Pd@ZIF-8 hollow microspheres. The shell thickness of ZIF-8 is about 180 nm.

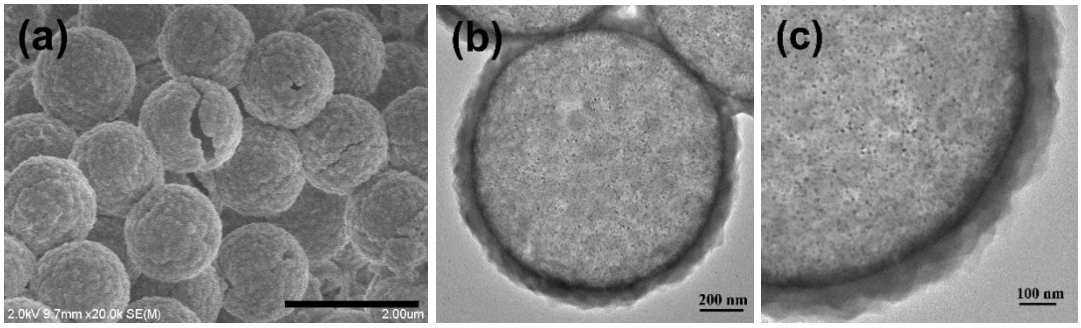

Figure 5. SEM image (a) and TEM images (b and c) of the Pd@ZIF-8 hollow microspheres with the diameter of Pd NPs being *ca.* 7.0 nm.

In addition, our convenient synthetic approach provides easy control of structural parameters of Pd@ZIF-8 hollow microspheres. Previous reports have demonstrated that, increased shell thickness of MOF in the structures of NM NPs encapsulated in MOF-based hollow structure leads to lower catalytic activity of NM NPs accompanied by sometimes enhanced selectivity.[31-33] This change is expected due to the slower diffusion of reactant and product associated with thicker shell of MOF. Therefore, the shell thickness can act as a regulator in the catalysis property. This regulating effect of thickness control has motivated us to explore the possibility for tailoring the shell thickness of ZIF-8 via our method. The shell thickness of ZIF-8 can be readily adjusted by varying the concentration of precursors while keeping the molar ratio between 2-methylimidazole

and zinc nitrate constant. Increasing the concentration of precursors resulted in the formation of ZIF-8 shell having a thickness of ~180 nm (Figure 4). Furthermore, the Pd NPs with larger size (*ca.* 7.0 nm) were successfully incorporated into the ZIF-8 hollow microspheres (Figure 5), by reducing the concentration of PS template microspheres that was added in $PdCl_2$ aqueous solution during the synthesis of Pd NPs.[20] The first step in the synthetic approach (Scheme 1) is based on our reported work on surface-assisted growth of Pd NPs on PS microspheres. Therein, the PS/Pd composite particles with smaller Pd NPs were found to exhibit higher catalytic activity. Since the Pd NPs function as the catalytically active component in the Pd@ZIF-8 hollow microspheres, we speculate the size adjustment of Pd NPs could also provide a regulation of their potential catalytic activity. Notably, our approach can also be used for encapsulating Ag NPs into ZIF-8 hollow microspheres (Figure 6), showing certain extendability. Uniform Ag NPs with an average particle size of about 45 nm were immobilized well on the inner surface of the ZIF-8 hollow microspheres. The resultant Ag@ZIF-8 hollow microspheres are envisaged to hold potential in several catalytic reactions, including the electrocatalytic reduction of hydrogen peroxide and carboxylation of terminal alkynes with CO_2.[34, 35]

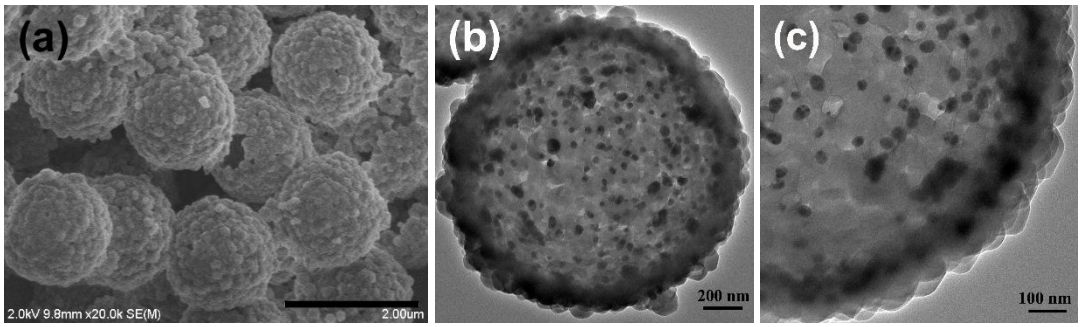

Figure 6. SEM image (a) and TEM images (b and c) of Ag@ZIF-8 hollow microspheres with the diameter of Ag NPs being *ca.* 45 nm.

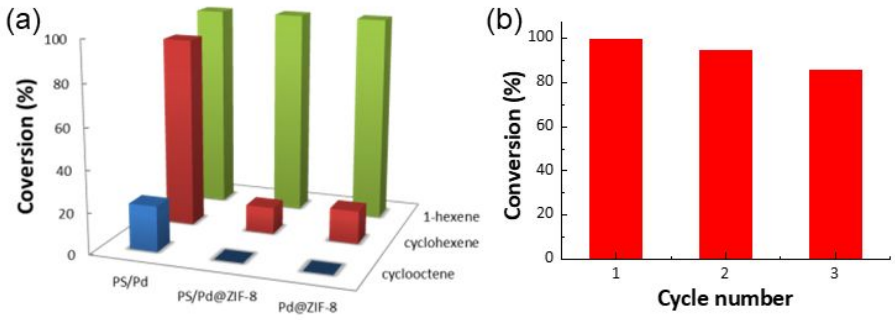

Figure 7. (a) Catalytic performance of PS/Pd composite particles, PS/Pd@ZIF-8 composite particles and Pd@ZIF-8 hollow microspheres for the hydrogenation of 1-hexene, cyclohexene and cyclooctene in liquid phase. Reaction time: 4 h for 1-hexene and cyclohexene, and 24 h for cyclooctene. (b) Recycling stability of Pd@ZIF-8 hollow microspheres in the hydrogenation of 1-hexene.

The liquid-phase hydrogenations of alkenes with different molecular sizes were carried out to assess the catalytic activity and selectivity of Pd@ZIF-8 hollow microspheres. For comparison, the PS/Pd and PS/Pd@ZIF-8 composite particles were also tested in the control experiments under the same conditions. A series of reaction results are presented in Figure 7. In the case of 1-hexene hydrogenation, all three different catalyst particles exhibit high catalytic activity and complete conversion of 1-hexene can be achieved in 4 h. This is because 1-hexene is small enough (2.5 Å), for diffusing through the pore apertures of ZIF-8 shell (3.4 Å) without hindrance.[13] As shown in Table 1, our Pd@ZIF-8 hollow microspheres exhibit high catalytic activity, that is comparable with a majority of the previous studies.[15, 25, 33, 36-38] As for the hydrogenation of cyclohexene (4.2 Å), the PS/Pd composite particles could still display good activity with conversion exceeding 90% in 4 h, while a drastic decrease in conversion was observed using the PS/Pd@ZIF-8 composite particles (13%) and Pd@ZIF-8 hollow microspheres (16%) as catalysts, respectively. Interestingly,

that cyclohexene could diffusion through the shells of ZIF-8, although the molecular size of cyclohexene exceeded the aperture size of ZIF-8. This phenomenon is derived from the framework flexibility of ZIF-8.[39, 40] More specifically, 2-methylimidazole ligands tend to undergo rotation under pressure or the introduction of guest molecules at room temperature, leading the effective aperture size for molecular diffusion to be ranging from 4.0 to 4.2 Å. In the hydrogenation of cyclooctene, Pd@ZIF-8 hollow microspheres and PS/Pd@ZIF-8 composite particles displayed no detectable activity, although the reactions were carried out for 24 h. In contrast, the PS/Pd composite particles exhibited some activity with a conversion of about 22%. In contrary to the cyclohexene, the size of cyclooctene (5.5 Å) is greatly larger than the aperture size of ZIF-8, thus only PS/Pd composite particles with Pd NPs anchored on the surface of PS microspheres have catalytic activity for the hydrogenation of cyclooctene.[41, 42] These results clearly demonstrate the ZIF-8 shell with well-defined pore structures can play the role of molecular sieve for selective catalysis. For the Pd@ZIF-8 hollow microspheres, the lack of activity for the hydrogenation of cyclooctene also indicated that the ZIF-8 shell was crack-free and no Pd NPs were present on their outer surface, consistent with the observations by SEM and TEM.[33]

Table 1. Summary of reaction conditions and final conversions during the catalytic hydrogenation of 1-hexene by various Pd NP-based catalysts

Catalyst	C_{Pd}:$C_{1\text{-hexene}}$	d_{Pd} (nm)	Time (h)	Temperature (°C)	Pressure (MPa)	Conversion (%)	Ref.
Pd@ZIF-8 hollow microsphere	1:212	4.7	4	25	0.1	99	ours
Pd@ZIF-8 hollow nanosphere	1:100	5	24	25	1	100	15
Pd@ZIF-8 nanosphere	1:205	*ca.* 15	24	35	0.1	98	33
Pd@ZIF catalyst	1:360	3 - 10	4	35	0.1	89.7	36
Void@HKUST-1/Pd@ZIF-8	1:851	*ca.* 10 - 20	0.08	25	1	83	37

yolk-shell Pd@ZIF-8 nanoparticle	1:1250	26	24	25	0.1	99	25
Pd/F-ZnO@ZIF-8	1:3000	5	10	35	0.1	100	38

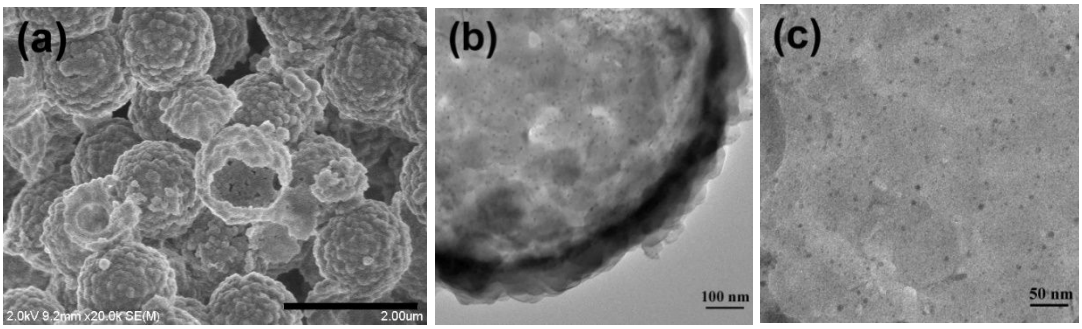

Figure 8. SEM image (a) and TEM images (b and c) of Pd@ZIF-8 hollow microspheres after three catalytic cycles.

The reusability of catalysts also represents an important property for exploring their practical uses. Figure 7b shows the stability of the Pd@ZIF-8 hollow microspheres in three consecutive cycles of 1-hexene hydrogenation. Obviously, the Pd@ZIF-8 hollow microspheres maintained their activity well and the conversion of 1-hexene dropped only slightly in each cycle. The SEM image indicated that the morphology of Pd@ZIF-8 hollow microspheres remained almost unchanged after three cycles, except for few broken ones, which may result from the stirring during the reaction (Figure 8a). TEM images show that there is almost no aggregation of the Pd NPs after reuse (Figure 8b and 8c). Moreover, the Pd content inside the Pd@ZIF-8 hollow microspheres was about 1.82% determined by ICP-OES. Therefore, the slight decrease in conversion can be ascribed to the loss of particulate catalyst during separation. In addition, the adsorption of reactant and product molecules in the micropores was also possible since no post-treatment was applied to the Pd@ZIF-8 hollow microspheres.

CONCLUSIONS

In summary, we have demonstrated a facile and sustainable strategy for fabricating Pd@ZIF-8 hollow microspheres with highly dispersed and small Pd NPs encapsulated within one ZIF-8 microsphere. The PVP-stabilized PS microspheres functioned as carriers for accommodating Pd NPs alongside the ZIF-8 shell, as well as the sacrificial template to produce interior cavity inside the ultimate Pd@ZIF-8 hollow microspheres. Notably, additional steps of surface treatments of as-prepared template microspheres are eliminated owing to the judicious selection of PVP-PS microspheres as templates. The as-prepared Pd@ZIF-8 hollow microspheres are uniform in size and have tailorable shell thicknesses, coupled with good structural stability. These unique structural advantages provide them with high catalytic activity, excellent size selectivity in the hydrogenation of alkenes and good stability in the recycling experiments. In addition, our strategy can be easily extended to the preparation of other NM@MOF (e.g. Ag@ZIF-8) hollow microspheres for wide-ranging potential applications.

ASSOCIATED CONTENT

Supporting Information

SEM and TEM images of PS microsphere; FTIR spectra of PS microspheres, PS/Pd composite particles, PS/Pd@ZIF-8 composite particles, Pd@ZIF-8 hollow microspheres, and pure ZIF-8; N2 adsorption/desorption isotherms and pore size distribution of pure ZIF-8.

AUTHOR INFORMATION

Corresponding Author

E-mail: yunxingli@jiangnan.edu.cn & tongai@cuhk.edu.hk

ORCID

Yunxing Li: 0000-0001-8532-2006

To Ngai: 0000-0002-7207-6878

NOTES

The authors declare no competing financial interest.

ACKNOWLEDGEMENTS

We would like to thank funding support from the National Natural Science Foundation of China (no. 21204030), the Fundamental Research Funds for the Central Universities (JUSRP21937, JUSRP11710), and MOE&SAFEA for the 111 Project (B13025).

REFERENCES

1. Xu, Y.; Chen, L.; Wang, X.; Yao, W.; Zhang, Q., Recent advances in noble metal based composite nanocatalysts: colloidal synthesis, properties, and catalytic applications. *Nanoscale* **2015**, *7*, 10559-10583.

2. Zaera, F., Nanostructured materials for applications in heterogeneous catalysis. *Chem. Soc. Rev.* **2013**, *42*, 2746-2762.

3. Yang, Q.; Xu, Q.; Jiang, H.-L., Metal-organic frameworks meet metal nanoparticles: synergistic effect for enhanced catalysis. *Chem. Soc. Rev.* **2017**, *46*, 4774-4808.

4. Chen, L.; Chen, H.; Li, Y., One-pot synthesis of Pd@MOF composites without the addition of stabilizing agents. *Chem. Commun.* **2014**, *50*, 14752-14755.

5. Chen, L.; Chen, H.; Luque, R.; Li, Y., Metal-organic framework encapsulated Pd nanoparticles: towards advanced heterogeneous catalysts. *Chem. Sci.* **2014**, *5*, 3708-3714.

6. Li, G.; Zhao, S.; Zhang, Y.; Tang, Z., Metal-organic frameworks encapsulating active nanoparticles as emerging composites for catalysis: recent progress and perspectives. *Adv. Mater.* **2018**, *30*, No. 1800702.

7. Liu, Y.; Liu, Z.; Huang, D.; Cheng, M.; Zeng, G.; Lai, C.; Zhang, C.; Zhou, C.; Wang, W.; Jiang, D.; Wang, H.; Shao, B., Metal or metal-containing nanoparticle@MOF nanocomposites as a promising type of photocatalyst. *Coord. Chem. Rev.* **2019**, *388*, 63-78.

8. Yang, Q.; Yao, F.; Zhong, Y.; Chen, F.; Shu, X.; Sun, J.; He, L.; Wu, B.; Hou, K.; Wang, D.; Li, X., Metal-organic framework supported palladium nanoparticles: applications and mechanisms. *Part. Part. Syst. Char.* **2019**, *36*, No. 1800557.

9. Aijaz, A.; Zhu, Q.-L.; Tsumori, N.; Akita, T.; Xu, Q., Surfactant-free Pd nanoparticles immobilized to a metal-organic framework with size- and location-dependent catalytic selectivity. *Chem. Commun.* **2015**, *51*, 2577-2580.

10. Osterrieth, J. W. M.; Wright, D.; Noh, H.; Kung, C.-W.; Vulpe, D.; Li, A.; Park, J. E.; Van Duyne, R. P.; Moghadam, P. Z.; Baumberg, J. J.; Farha, O. K.; Fairen-Jimenez, D., Core-shell gold nanorod@zirconium-based metal-organic framework composites as in situ size-selective raman probes. *J. Am. Chem. Soc.* **2019**, *141*, 3893-3900.

11. Liu, Y.; Zhang, J.; Song, L.; Xu, W.; Guo, Z.; Yang, X.; Wu, X.; Chen, X., Au-HKUST-1 composite nanocapsules: synthesis with a coordination replication strategy and catalysis on CO oxidation. *ACS Appl. Mater. Interfaces* **2016**, *8*, 22745-22750.

12. Lu, G.; Li, S.; Guo, Z.; Farha, O. K.; Hauser, B. G.; Qi, X.; Wang, Y.; Wang, X.; Han, S.; Liu, X.; DuChene, J. S.; Zhang, H.; Zhang, Q.; Chen, X.; Ma, J.; Loo, S. C. J.; Wei, W. D.; Yang, Y.; Hupp, J. T.; Huo, F., Imparting functionality to a metal-organic framework material by controlled nanoparticle encapsulation. *Nat. Chem.* **2012**, *4*, 310-316.

13. Park, K. S.; Ni, Z.; Cote, A. P.; Choi, J. Y.; Huang, R.; Uribe-Romo, F. J.; Chae, H. K.; O'Keeffe, M.; Yaghi, O. M., Exceptional chemical and thermal stability of zeolitic imidazolate frameworks. *Proc. Natl. Acad. Sci. U.S.A.* **2006**, *103*, 10186-10191.

14. Qian, X.; Sun, F.; Sun, J.; Wu, H.; Xiao, F.; Wu, X.; Zhu, G., Imparting surface hydrophobicity to metal-organic frameworks using a facile solution-immersion process to enhance water stability for CO_2 capture. *Nanoscale* **2017**, *9*, 2003-2008.

15. Wang, X.; Li, M.; Cao, C.; Liu, C.; Liu, J.; Zhu, Y.; Zhang, S.; Song, W., Surfactant-free palladium nanoparticles encapsulated in ZIF-8 hollow nanospheres for size-selective catalysis in liquid-phase solution. *Chemcatchem* **2016**, *8*, 3224-3228.

16. Sisman, T., Early life stage and genetic toxicity of stannous chloride on zebrafish embryos and adults: toxic effects of tin on zebrafish. *Environ. Toxicol.* **2011**, *26*, 240-249.

17. Dantas, F. J. S.; de Mattos, J. C. P.; Moraes, M. O.; Viana, M. E.; Lage, C. A. S.; Cabral-Neto, J. B.; Leitao, A. C.; Bernardo, M.; Bezerra, R.; Carvalho, J. J.; Caldeira-de-Araujo, A., Genotoxic effects of stannous chloride ($SnCl_2$) in K562 cell line. *Food Chem. Toxicol.* **2002**, *40*, 1493-1498.

18. Cowell, E. M., Chemical warfare and the doctor-I. *Br Med J* **1939**, *2*, 736-8.

19. Xiong, Y.; Washio, I.; Chen, J.; Cai, H.; Li, Z.-Y.; Xia, Y., Poly(vinyl pyrrolidone): a dual functional reductant and stabilizer for the facile synthesis of noble metal nanoplates in aqueous solutions. *Langmuir* **2006**, *22*, 8563-8570.

20. Zhao, Y.; Feng, J.; Hong, L.; Li, Y.; Wang, C.; Ye, S., Simple surface-assisted formation of palladium nanoparticles on polystyrene microspheres and their application in catalysis. *Inorg. Chem. Front.* **2018**, *5*, 1133-1138.

21. Zhang, M.; Yang, Y.; Li, C.; Liu, Q.; Williams, C. T.; Liang, C., PVP-Pd@ZIF-8 as highly efficient and stable catalysts for selective hydrogenation of 1,4-butynediol. *Catal. Sci. Technol.* **2014**, *4*, 329-332.

22. Lee, H. J.; Cho, W.; Oh, M., Advanced fabrication of metal-organic frameworks: template-directed formation of polystyrene@ZIF-8 core-shell and hollow ZIF-8 microspheres. *Chem. Commun.* **2012**, *48*, 221-223.

23. Tang, J.; Salunkhe, R. R.; Liu, J.; Torad, N. L.; Imura, M.; Furukawa, S.; Yamauchi, Y., Thermal conversion of core-shell metal-organic frameworks: a new method for selectively functionalized nanoporous hybrid carbon. *J. Am. Chem. Soc.* **2015**, *137*, 1572-1580.

24. Ni, X.; Hao, J.; Zhao, Y.; Yang, C.; Sun, P.; Wang, C.; Li, Y., A simple and general approach for the decoration of interior surfaces of silica hollow microspheres with noble metal nanoparticles and their application in catalysis. *Inorg. Chem. Front.* **2017**, *4*, 1634-1641.

25. Li, F.-L.; Li, H.-X.; Lang, J.-P., Fabrication of yolk-shell Pd@ZIF-8 nanoparticles with excellent catalytic size-selectivity for the hydrogenation of olefins. *Crystengcomm* **2016**, *18*, 1760-1767.

26. Lin, L.; Zhang, T.; Liu, H.; Qiu, J.; Zhang, X., In situ fabrication of a perfect Pd/ZnO@ZIF-8 core-shell microsphere as an efficient catalyst by a ZnO support-induced ZIF-8 growth strategy. *Nanoscale* **2015**, *7*, 7615-7623.

27. Zhu, H.; Zhang, Q.; Zhu, S., Preparation of raspberry-like ZIF-8/PS composite spheres via dispersion polymerization. *Dalton Trans.* **2015**, *44*, 16752-16757.

28. Zhang, N.; Xu, Y.-J., Aggregation- and Leaching-Resistant, Reusable, and Multifunctional Pd@CeO_2 as a Robust Nanocatalyst Achieved by a Hollow Core-Shell Strategy. *Chem. Mater.* **2013**, *25*, 1979-1988.

29. Zhang, N.; Liu, S.; Fu, X.; Xu, Y.-J., Fabrication of coenocytic Pd@CdS nanocomposite as a visible light photocatalyst for selective transformation under mild conditions. *J. Mater. Chem.* **2012**, *22*, 5042-5052.

30. Yang, Q.; Xu, Q.; Yu, S.-H.; Jiang, H.-L., Pd nanocubes@ZIF-8: integration of plasmon-driven photothermal conversion with a metal-organic framework for efficient and selective catalysis. *Angew. Chem. Int. Ed.* **2016**, *55*, 3685-3689.

31. Zhao, M. T.; Yuan, K.; Wang, Y.; Li, G. D.; Guo, J.; Gu, L.; Hu, W. P.; Zhao, H. J.; Tang, Z. Y., Metal-organic frameworks as selectivity regulators for hydrogenation reactions. *Nature* **2016**, *539*, 76-80.

32. Zhang, T.; Zhang, X. F.; Yan, X. J.; Lin, L.; Liu, H. O.; Qiu, J. S.; Yeung, K. L., Core-shell Pd/ZSM-5@ZIF-8 membrane micro-reactors with size selectivity properties for alkene hydrogenation. *Catal. Today* **2014**, *236*, 41-48.

33. Yang, Y.; Wang, F.; Yang, Q.; Hu, Y.; Yan, H.; Chen, Y.-Z.; Liu, H.; Zhang, G.; Lu, J.; Jiang, H.-L.; Xu, H., Hollow metal-organic framework nanospheres via emulsion-based interfacial synthesis and their application in size-selective catalysis. *ACS Appl. Mater. Interfaces* **2014**, *6*, 18163-18171.

34. Dong, Y. H.; Duan, C. Q.; Sheng, Q. L.; Zheng, J. B., Preparation of Ag@zeolitic imidazolate framework-67 at room temperature for electrochemical sensing of hydrogen peroxide. *Analyst*, **2019**, *144*, 521-529.

35. Shi, J. L.; Zhang, L. N.; Sun, N. N.; Hu, D.; Shen, Q.; Mao, F.; Gao, Q.; Wei, W., Facile and rapid preparation of Ag@ZIF-8 for carboxylation of terminal alkynes with CO_2 in mild conditions. *ACS Appl. Mater. Interfaces* **2019**, *11*, 28858-28867.

36. Ding, S. S.; Yan, Q.; Jiang, H.; Zhong, Z. X.; Chen, R. Z.; Xing, W. H., Fabrication of Pd@ZIF-8 catalysts with different Pd spatial distributions and their catalytic properties. *Chem. Eng. J.*, **2016**, *296*, 146-153.

37. Wan, M. M.; Zhang, X. L.; Li, M. Y.; Chen, B.; Yin, J.; Jin, H. C.; Lin, L.; Chen, C.; Zhang, N., Hollow Pd/MOF nanosphere with double shells as multifunctional catalyst for hydrogenation reaction. *Small* **2017**, *13*, 1701395.

38. Lin, L.; Liu, H. O.; Zhang, X. F., Flower-like ZnO-assisted one-pot encapsulation of noble metal nanoparticles supported catalysts with ZIFs. *Appl. Surf. Sci.*, **2018**, *433*, 602-609.

39. Fairen-Jimenez, D.; Moggach, S. A.; Wharmby, M. T.; Wright, P. A.; Parsons, S.; Dueren, T., Opening the gate: framework flexibility in ZIF-8 explored by experiments and simulations. *J. Am. Chem. Soc.* **2011**, *133*, 8900-8902.

40. Kuo, C.-H.; Tang, Y.; Chou, L.-Y.; Sneed, B. T.; Brodsky, C. N.; Zhao, Z.; Tsung, C.-K., Yolk-shell nanocrystal@ZIF-8 nanostructures for gas-phase heterogeneous catalysis with selectivity control. *J. Am. Chem. Soc.* **2012**, *134*, 14345-14348.

41. Yin, H.; Choi, J.; Yip, A. C. K., Anti-poisoning core-shell metal/ZIF-8 catalyst for selective alkene hydrogenation. *Catal. Today* **2016**, *265*, 203-209.

42. Lin, L.; Zhang, T.; Zhang, X.; Liu, H.; Yeung, K. L.; Qiu, J., New Pd/SiO_2@ZIF-8 Core-shell catalyst with selective, antipoisoning, and antileaching properties for the hydrogenation of alkenes. *Ind. Eng. Chem. Res.* **2014**, *53*, 10906-10913.

Table of Content